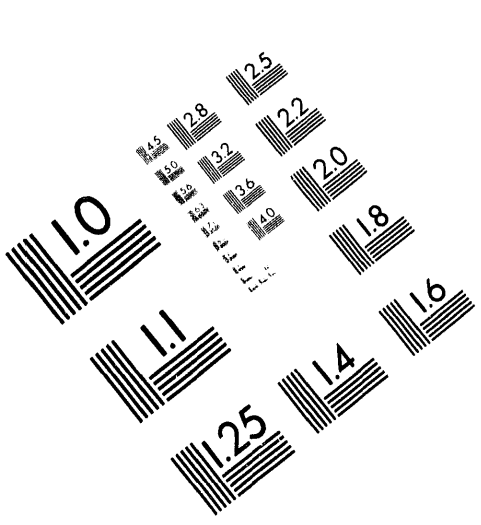

Association for Information and Image Management
1100 Wayne Avenue, Suite 1100
Silver Spring, Maryland 20910
301/587-8202

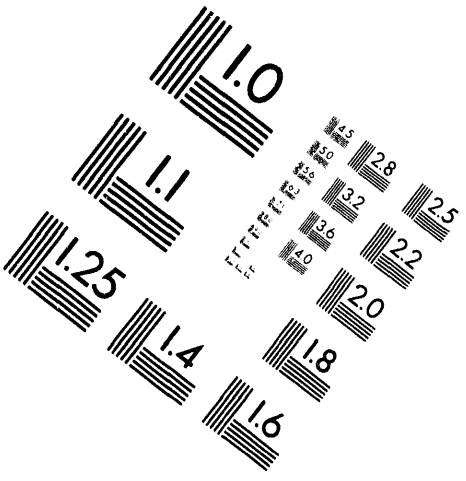

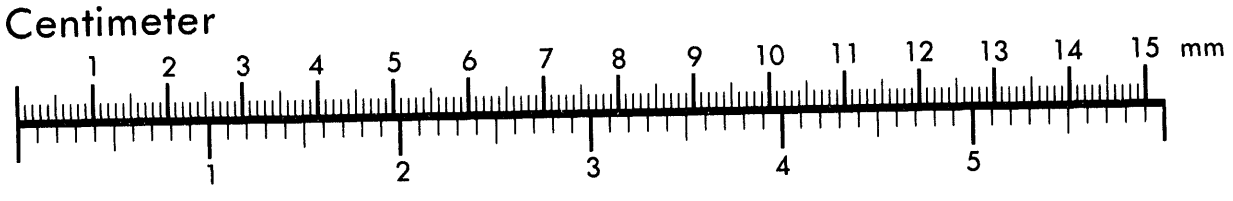

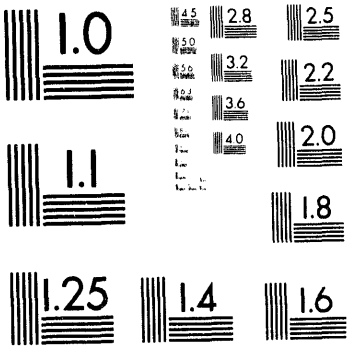

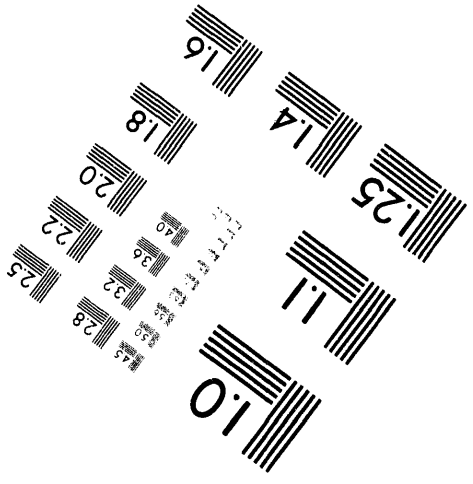

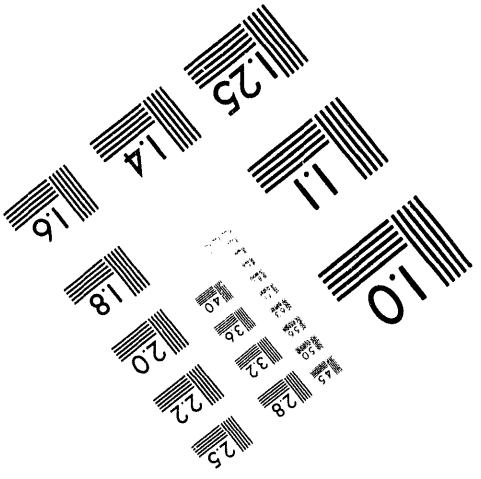

1 of 1

SAND94-0273C
Conf-9405158--1

The Non-Proliferation Experiment recorded at the Pinedale Seismic Research Facility

Dorthe B. Carr
Sandia National Laboratories
Seismic Verification Technologies Department
Albuquerque, New Mexico 87185-0655

Abstract

The Non-Proliferation Experiment was recorded by five different seismic stations operated by Sandia National Laboratories at the Pinedale Seismic Research Facility, approximately 7.6° from the Nevada Test Site. Two stations are different versions of the Deployable Seismic Verification System developed by the Department of Energy to provide seismic data to verify compliance with a Comprehensive Test Ban Treaty. Vault and borehole versions of the Designated Seismic Stations also recorded the event. The final station is test instrumentation located at depths of 10, 40 and 1200 feet. Although the event is seen clearly at all the stations, there are variations in the raw data due to the different bandwidths and depths of deployment.

One Deployable Seismic Verification System has been operating at Pinedale for over three years and in that time recorded 14 nuclear explosions and 4 earthquakes from the Nevada Test Site, along with numerous other western U. S. earthquakes. Several discriminants based on the work by Taylor et al. (1989) have been applied to this data. First the discriminants were tested by comparing the explosions only to the 4 earthquakes located on the Test Site. Only one discriminant, $log(L_g/P_g)$, did not show clear separation between the earthquakes and nuclear explosions. When other western U. S. events are included, only the m_b vs. M_s discriminant separated the events. In all cases where discrimination was possible, the Non-Proliferation Experiment was indistinguishable from a nuclear explosion.

Text of Presentation

The Pinedale Seismic Research Facility (PSRF) operated by the Air Force Technical Applications Center (AFTAC) is located in western Wyoming on the western front of the Wind River Mountains. PSRF is approximately 7.5-7.6° (830-850 km) from the northern end of the Nevada Test Site (NTS) (Figure 1). At the time of the Non-Proliferation Experiment (NPE) on September 22, 1993, Sandia National Laboratories was operating five stations at PSRF (Table 1). Two of the stations were different configurations of the Deployable Seismic Verification System (DSVS), developed for use with a Comprehensive Test Ban Treaty. A DSVS using the RSS3 configuration was installed in the spring of 1990. This configuration uses two Teledyne-Geotech seismometers, a S3 and a 54000, in two boreholes to record three component data between 0.01 and 50 Hz. The second DSVS with the RSS1 configuration, records three component data with a Guralp CMG-3 seismometer from 0.05 to 30 Hz. Both systems have

the seismometers at a depth of 40 feet. Two Designated Seismic Stations (DSS) were deployed at PSRF for four days around the NPE. DSS was developed for use with the Threshold Test Ban Treaty signed with the former Soviet Union. One DSS was in a borehole at approximately 100 meters and the other was in a vault around 8-10 feet deep. Both systems use Teledyne-Geotech seismometers and record three component data from 0.1 to 10 Hz. The last system operating at PSRF during the NPE is being used in an experiment to look at how noise varies with depth at PSRF. Three vertical seismometers, two Teledyne-Geotech GS13 and one Teledyne Geotech GS28, were deployed at different depths. One GS13 was in a shallow vault at 10 feet, and the other was in a deep vault at 40 feet. The GS28 was in a borehole at a depth of 1200 feet. All three seismometers recorded data from 1 to 50 Hz.

All of the stations recorded good data from the NPE (Figures 2-5). Figure 2 shows the vertical traces from the two DSVS stations (HF band, 0.5-50.0/30.0 Hz), the deep borehole at 1200 feet and the vault and borehole systems of DSS. All the traces are independently scaled so that the signals can be seen. The DSS instruments amplitudes are larger than the other three instruments by roughly a factor of 10^6. The amplitude of the signal from deep borehole instrument is about a factor of 5 higher than the DSVS stations. The P_n arrival comes in clearly, with the first motion being down. All five traces have very similar signals when plotted out to see the first thirty seconds (Figure 3). The DSS stations were located approximately 1.5 miles from the other three systems, so the slight differences in the signals from DSS are most probably due to a combination of bandwidth and local geology. The P_g arrival should come in near 27 seconds, and although there is an increase in amplitude at this time (Figure 2), there is no clear onset of the P_g wave. There is no S_n arrival, which is not unusual in the western United States (WUS). The L_g arrival comes in clearly, especially on the deep borehole, DSS (Figure 5) and the IP band (0.01-2.5 Hz) of DSVS when high pass filtered. There are no clear surface waves on the LP band (0.02-0.05 Hz) of DSVS/RSS3 (Figure 4).

The signal to noise ration (SNR) of the Pn wave was greater than 12 dB for frequencies between 0.6 and 3.2 Hz. Out to 7.5 Hz, the SNR was still more than 2 dB. The signal went into the background noise at 9.5 Hz. A backazimuth for the NPE was calculated on DSVS/RSS3 using the three component method by Magotra et al. (1987). The backazimuth calculated was 206.4 °, which is off by almost 19°. Two other NTS nuclear explosions, Mineral Quarry and Hunter's Trophy, were located close to the NPE. Calculated backazimuths for these two events were off by 5° and 13.5° respectively. An "array" backazimuth calculation using the five stations operating at PSRF for the NPE is not possible because of the timing on the DSS stations.

Sandia National Laboratories installed the first DSVS station (RSS3 configuration) in the spring of 1990. In the two and one half years the data was transmitted by satellite to Albuquerque, a good database of events occurring in the WUS was collected. Some of these events have been used to look at discrimination between earthquakes, nuclear explosions and the NPE at PSRF (Table 2, 3; Figure 6). Fourteen NTS nuclear explosions were recorded at PSRF, plus four earthquakes that occurred on or close

to the test site with NEIS body-wave magnitudes between 3.8 and 5.6. Twenty-nine other WUS earthquakes at distances between 236 and 1290 km from PSRF were also collected for the study (Table 3). The event from South Dakota (5-Nov-1991) was classified as a rockburst in the PDE bulletin. Finally, a DOD explosion at White Sands, NM on 20-Jun-1991 was also included in the data base.
Traces from the NPE, Hunter's Trophy and EQ #2 are in Figure 7. All these events had similar magnitudes in the PDE bulletin. There is much more L_g energy in the EQ #2 trace than for either explosion. Figure 8 shows the first 30 seconds of the NPE and Hunter's Trophy. The signals, especially in the first three to five seconds, look very similar at PSRF. Both of these explosions come from similar locations at the Test Site (Table 2). The discriminants used in the study are based on work done by Taylor et al. (1989) at the LLNL seismic network around NTS. Only discriminants that worked fairly well in that study were tried at PSRF: m_b vs. M_s, m_b vs. M_s^h, $log(L_g/P_g)$, corner frequency and spectral ratios. Table 4 documents the methods used to calculate the discriminants.

The results of the discrimination studies can be seen in Figures 9 through 18. Figure 9 shows m_b vs. M_s for eleven NTS explosions, the four earthquakes on NTS and the NPE. There is good separation using this discriminant between nuclear explosions and earthquakes located on the Test Site. At this regional distance and test site, the NPE is indistinguishable from a nuclear explosion. Figure 10 is the same data as in Figure 9, plus the 29 WUS earthquakes and DOD explosion at White Sands. There is still fairly good separation between the explosions and earthquakes. Two earthquakes with m_b between 3.3 and 3.5 fall on the explosion side. They are the Wyoming earthquakes of 13-Apr-1991 and 02-Nov-1992 (Table 3).

The Forsyth (1976) M_s^h measures higher-mode surface waves earlier in the trace (Table 4). Figures 11 and 12 show m_b vs. M_s^h for only the NTS events and for all WUS events, respectively. There is good separation using this discriminant between nuclear explosions and earthquakes located at the Test Site. Again, the NPE is indistinguishable from a nuclear explosion. When WUS events are added (Figure 12), there is still fairly good separation between explosions and earthquakes for higher magnitude events. At $m_b < 3.6$, the discriminant breaks down, partly because there are no nuclear explosions at these magnitudes to compare to the WUS earthquakes.

Figure 13 shows the $log(L_g/P_g)$ discriminant for all fourteen nuclear explosions, the four NTS earthquakes and the NPE. There is not a clear separation between earthquakes and explosions for this discriminant. The attenuation of higher frequency (> 8 Hz) energy and the recording site geology probably contribute to the "failure" of this discriminant. The data using all WUS events is in Figure 14.

Corner frequencies were calculated for eleven of the NTS nuclear explosions, the four earthquakes on NTS, the NPE and eleven WUS earthquakes with body-wave magnitudes in the PDE bulletin. Figure 15 shows the corner frequencies for all the events from NTS. There is good separation between the earthquakes and explosions, and the NPE is again indistinguishable from a nuclear explosion.

The other WUS earthquakes have corner frequencies similar to the nuclear explosion (Figure 16). It appears that the NTS earthquakes have unusually low corner frequencies at PSRF.

Spectral ratio discriminants work best if the two frequency bands are not close together. At PSRF we are limited by the fact that the majority of events have signal going into the background noise between 7 and 10 Hz. In Figure 17 are the spectral ratios using 0.4-0.6 Hz over 4.0-6.0 Hz for all the events from NTS. There is no distance correction on this plot, since all the events are from the same area. The earthquakes and explosions separate using this discriminant and again, at this distance and test site the NPE is indistinguishable from a nuclear explosion. The WUS events are added in Figure 18 and a first order distance correction applied to the data. After adding in these earthquakes, there is no clear separation between earthquakes and explosions using spectral ratios.

Conclusion

The Non-Proliferation Experiment was recorded well at PSRF by all five systems Sandia National Laboratories was operating. The character of the seismic trace was similar to Hunter's Trophy, a nuclear explosion of similar size and location. All the regional discriminants tested with data from the DSVS/RSS3 located at PSRF worked for nuclear explosions and earthquakes located on or near NTS, except for $log(L_g/P_g)$. In all cases, the NPE was indistinguishable from the nuclear explosions. When other WUS earthquakes are added, all the discriminants except m_b vs. M_s break down. Apparently for the other discriminants the path effects are very important.

Acknowledgments

This work was supported by the United States Department of Energy under Contract DE-AC04-94AL85000.

References

Evernden, J. F., (1967). Magnitude determination of regional and near-regional distances in the United States, *Bull. Seis. Soc. Am.*, **57**, 591-639.

Forsyth, D. W., (1976). Higher mode Rayleigh waves as an aid to seismic discrimination, *Bull. Seis. Soc. Am.*, **66**, 827-841.

Magotra, N., N. Ahmed and E. Chael, (1987). Seismic event detection and source location using single station (three-component) data, *Bull. Seis. Soc. Am.*, **77**, 958-971.

Marshall, P. D. and P. W. Basham, (1972). Discrimination between earthquakes and underground explosions employing an improved Ms scale, *Geophys. J. R. astr. Soc.*, **28**, 431-458.

Taylor, S. R., M. D. Denny, E. S. Vergino and R. E. Glaser, (1989). Regional discrimination between NTS explosions and western U. S. earthquakes, *Bull. Seis. Soc. Am.*, **79**, 1142-1176.

Figure 11. The discriminant m_b vs. M_s^h for events located on NTS.

Figure 12. The discriminant m_b vs. M_s^h for events shown in Figure 11, plus other WUS earthquakes.

Figure 13. The discriminant m_b vs. *log* (L_g/P_g) for events located on NTS.

Figure 14. The discriminant m_b vs. *log* (L_g/P_g) for events shown in Figure 13, plus other WUS earthquakes.

Figure 15. The discriminant m_b vs. corner frequency for events located on NTS.

Figure 16. The discriminant m_b vs. corner frequency for events shown in Figure 15, plus other WUS earthquakes.

Figure 17. The discriminant m_b vs. spectral ratios for events located on NTS.

Figure 18. The discriminant m_b vs. spectral ratios for events shown in Figure 17, plus other WUS earthquakes.

Table 1: Specifics of seismic systems operating at PSRF

SYSTEM	SEISMOMETER(s)	DEPTH	FREQUENCY BAND
DSVS/RSS3	Teledyne Geotech S3	40 feet	0.01-50.0 Hz
	Teledyne Geotech 54000		
DSVS/RSS1	Guralp CMG-3	40 feet	0.05-30.0 Hz
DSS (borehole)	Teledyne Geotech S3	100 meters	0.1-10.0 Hz
DSS (vault)	Teledyne Geotech GS13		0.1-10.0 Hz
experimental	Teledyne Geotech GS13	10 feet	1.0-50.0 Hz
	Teledyne Geotech GS13	40 feet	1.0-50.0 Hz
	Teledyne Geotech GS28	1200 feet	1.0-50.0 Hz

Table 2: NTS explosions and earthquakes

NAME	DATE	LOCATION		DISTANCE	NEIS m_b
BULLION #	13-JUN-1991	37.262N	116.420W	846.7 km	5.7
MINERAL QUARRY #	25-JUL-1990	37.207N	116.214W	839.3 km	4.7
HOUSTON #	14-NOV-1990	37.227N	116.371W	846.7 km	5.4
BEXAR	04-APR-1991	37.296N	116.313W	837.6 km	5.6
MONTELLO	16-APR-1991	37.245N	116.442W	849.4 km	5.4
FLOYDATA	15-AUG-1991	37.087N	116.002W	837.6 km	4.2
HOYA	14-SEP-1991	37.226N	116.428W	850.1 km	5.5
DISTANT ZENITH	19-SEP-1991	37.236N	116.166W	834.1 km	4.0
LUBBOCK	18-OCT-1991	37.063N	116.045W	842.1 km	5.2
BRISTOL	26-NOV-1991	37.096N	116.070W	840.6 km	4.6
JUNCTION	26-MAR-1992	37.272N	116.360W	842.3 km	5.5
GALENA	23-JUN-1992	37.124N	116.031W	836.0 km	3.9*
HUNTER'S TROPHY	18-SEP-1992	37.207N	116.210W	839.1 km	4.4
DIVIDER	23-SEP-1992	37.021N	115.998W	843.1 km	4.4
NPE	22-SEP-1993	37.126N	116 159W	839.6 km	4.1
EQ #1	29-JUN-1992	36.705N	116.293W	886.9 km	5.6
EQ #2	29-JUN-1992	36.686N	116.238W	885.6 km	4.3
EQ #3	29-JUN-1992	36.756N	116.236W	885.2 km	3.8
EQ #4	28-JUN-1992	36.419N	116.780W	939.0 km	4.4

no IP or LP data for this event

* local magnitude

Table 3: Western United States events

STATE	DATE	LOCATION		DISTANCE	NEIS m_b
Utah	22-MAR-1991	37.816N	112.995W	623.9 km	3.2
California	24-MAR-1991	37.645N	118.945W	979.5 km	3.3
Wyoming	13-APR-1991	42.031N	106.857W	236.6 km	3.2
California	04-MAY-1991	37.552N	118.432W	951.2 km	4.1*
Colorado	10-MAY-1991	37.466N	106.594W	641.9 km	3.4*
Nevada	17-MAY-1991	39.194N	114.960W	603.6 km	3.2*
New Mexico %	20-JUN-1991	33.619N	106.475W	1053.2 km	3.5*
Montana	18-JUL-1991	47.753N	113.841W	646.7 km	3.5
California/Nevada	12-AUG-1991	38.220N	118.750W	927.2 km	4.4
Utah	21-AUG-1991	39.364N	111.878W	426.6 km	3.3*
South Dakota ^	05-NOV-1991	44.350N	103.750W	499.2 km	2.5*
Utah	21-DEC-1991	37.567N	112.322W	625.2 km	3.6
New Mexico	02-JAN-1992	32.347N	103.124W	1290.0 km	4.7
Idaho	24-JAN-1992	43.999N	113.893W	373.6 km	2.7
Idaho	07-MAR-1992	44.530N	114.125W	416.0 km	3.8*
Montana	21-MAR-1992	47.267N	113.295W	579.1 km	3.7
Idaho	22-MAR-1992	44.582N	114.185W	422.8 km	4.3*
Nevada	24-MAR-1992	39.425N	119.924W	944.5 km	3.4*
Utah	24-JUN-1992	38.783N	111.554W	474.9 km	4.4*
California	09-JUL-1992	34.239N	116.837W	1140.4 km	5.6
Utah	11-JUL-1992	39.322N	111.123W	406.1 km	3.9
California	11-JUL-1992	35.210N	118.066W	1116.4 km	5.3
Nevada	16-JUL-1992	38.323N	116.159W	745.6 km	3.1*
Nevada	17-JUL-1992	38.387N	116.120W	738.3 km	3.1*
Idaho	28-AUG-1992	44.583N	113.323W	363.4 km	3.4
Utah	02-SEP-1992	37.090N	113.472W	715.0 km	5.8
California	19-SEP-1992	38.863N	122.793W	1194.3 km	4.6
Wyoming	02-NOV-1992	42.740N	104.389W	421.7 km	3.0*
Nevada	10-DEC-1992	39.682N	115.956W	636.1 km	3.2*
Utah	18-DEC-1992	39.729N	110.838W	355.5 km	3.1

% DOD explosion
^ rockburst
* local magnitude

Table 4: Methods used to determine the discriminants used in the study

1. m_b was calculated using the WUS magnitude formula by Evernden (1967):

$$m_b = -7.55 + 1.21log(A/T) + 3.06log(\Delta)$$

A = 0 to peak amplitude (nm) measured in the time window from the initial onset to Δ/6.0 sec on HFZ
T = period (sec)
Δ = distance (km)
All the data was low-pass filtered at 4 Hz

2. M_s was calculated using the formula of Marshall and Basham (1972):

$$M_s = log\ (A) + B'(\Delta) + P(T)$$

A = 0 to peak amplitude (nm) measured in the time window Δ/3.1 to Δ/2.8 + 29.0 sec on LPZ
B'(Δ) = distance correction
P(T) = period-dependent path correction
For approximately all events with $m_b < 4.0$, Rayleigh waves were not seen clearly on LPZ, so M_s is an upper bound of the noise.

3. M_s^h was calculated using the formula by Forsyth (1976):

$$M_s^h = \log(A) + B'(\Delta) + \log(T/T_0) + \log(7.5)$$

A = maximum amplitude (nm) measured in the time window of Δ/4.0 to Δ/3.5 sec on IPZ
B'(Δ) = distance correction from Marshall and Basham (1972)
T = period (sec)
T_0 = 10 seconds

4. The maximum peak-to-peak amplitudes of L_g and P_g were measured on HFZ after low-pass filtering at 10 Hz. The amplitude of L_g was measured in the time window Δ/3.8 to Δ/3.0 seconds and the amplitude of P_g was measured in the time window Δ/6.0 to Δ/5.2 seconds.
5. Corner frequencies were found by calculating the displacement spectrum on the IPZ band and measuring the corner frequency by eye.
6. Spectral ratios were calculated by comparing the average value of displacement using two spectral windows: 0.4-0.6 Hz on IPZ and 4.0-6.0 Hz on HFZ. Ratios were made for P_n (initial onset to Δ/6.0 sec) and corrected for distance using a first-order correction.

Figure Captions

Figure 1. Map showing the location of the Pinedale Seismic Research Facility (PSRF) and the Nevada Test Site (NTS).

Figure 2. Vertical traces of the NPE from the stations operating at PSRF. The traces are independently scaled.

Figure 3. The first 30 seconds of the NPE as recorded at PSRF.

Figure 4. The vertical traces of the NPE on the three bands of DSVS/RSS3. The event is seen clearly on the IP band when high pass filtered at 0.5 Hz. There are no clear surface waves on the LP band.

Figure 5. The NPE on all three components of the DSS in the borehole. Note the good L_g arrival.

Figure 6. Map of the events used in the discrimination study at PSRF.

Figure 7. Vertical traces of the NPE, NTS explosion Hunter's Trophy and an earthquake at the southern end of NTS. The events have similar magnitudes. The traces are scaled relative to one another.

Figure 8. The first 30 seconds of the NPE and Hunter's Trophy for comparison.

Figure 9. The discriminant m_b vs. M_s for events located on NTS.

Figure 10. The discriminant m_b vs. M_s for events shown in Figure 9, plus other WUS earthquakes.

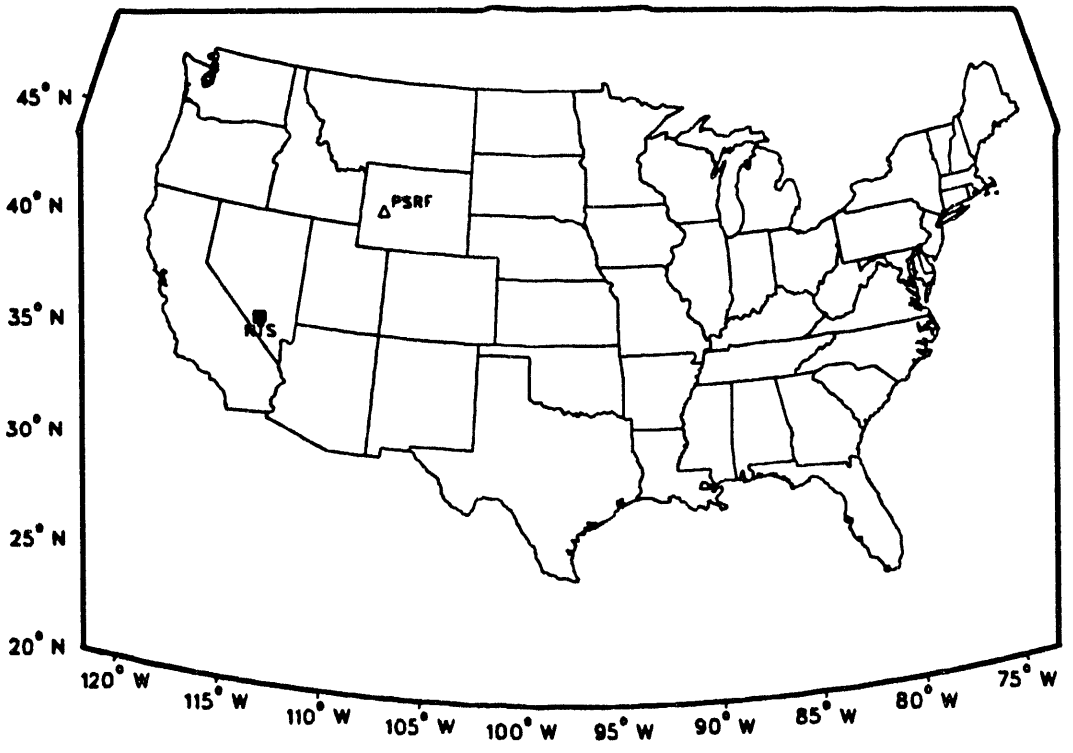
45° N
40° N
35° N
30° N
25° N
20° N
120° W
115° W
110° W
105° W
100° W
95° W
90° W
85° W
80° W
75° W
PSRF
RTS

Fig 1

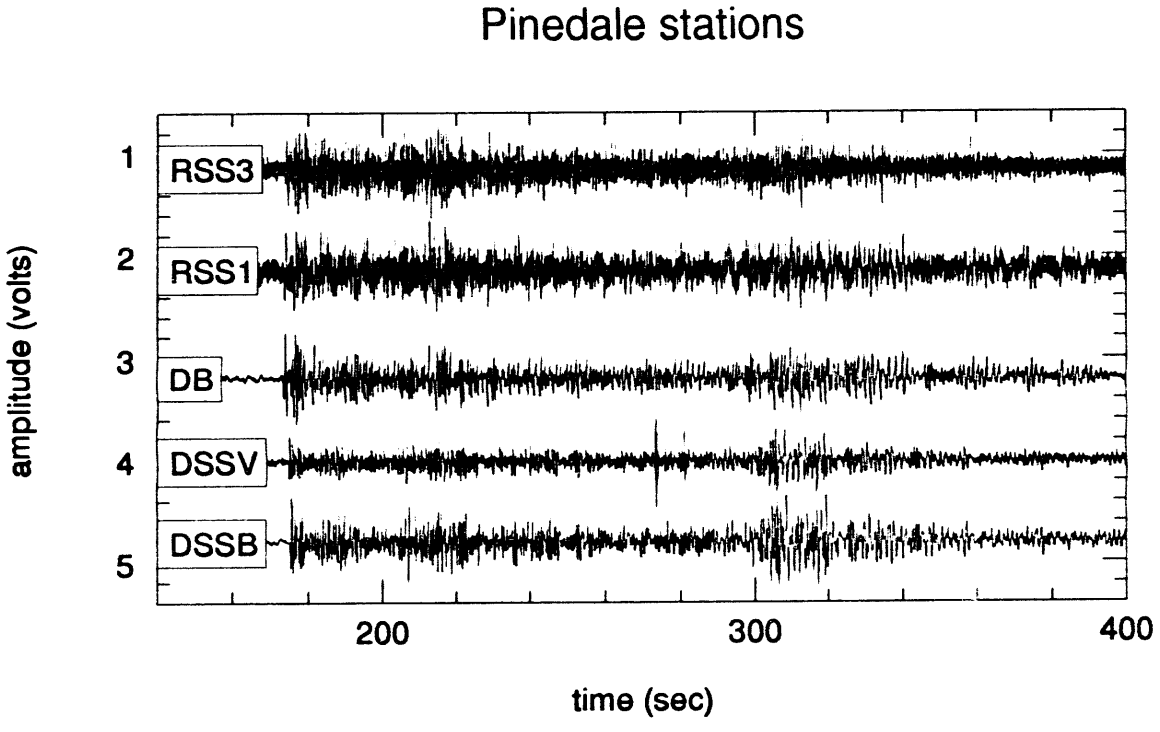
Pinedale stations
1
RSS3
2
RSS1
3
DB
4
DSSV
5
DSSB
amplitude (volts)
200
300
400
time (sec)

Fig 2

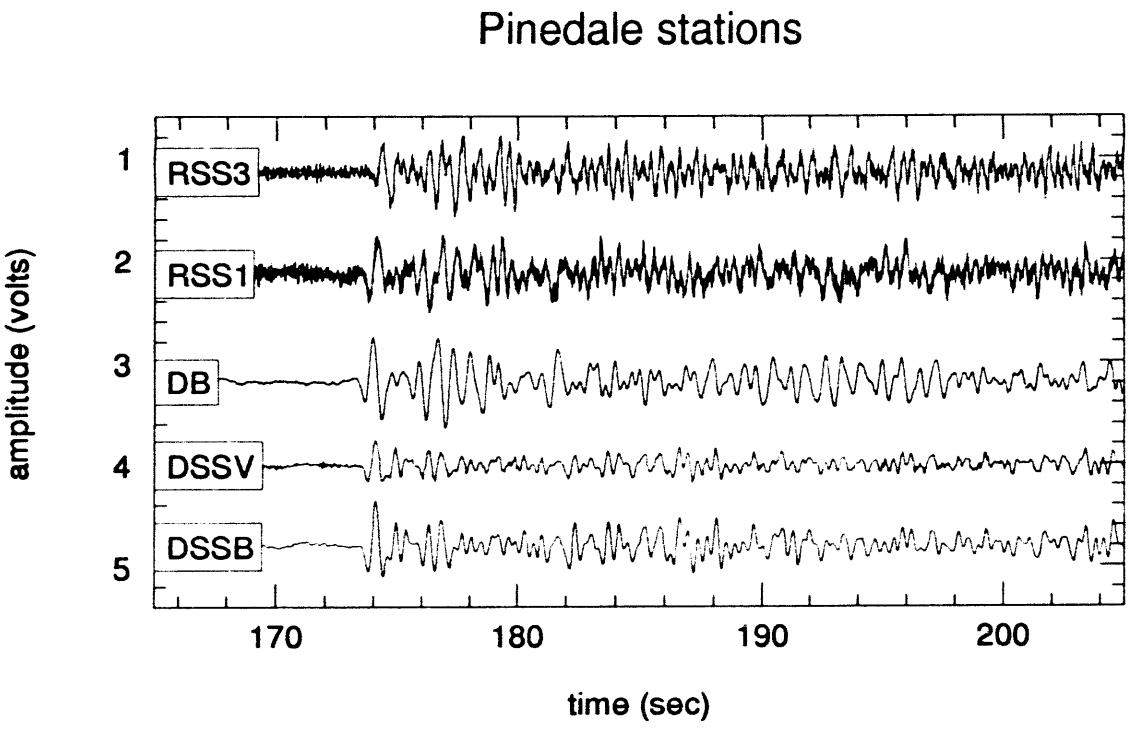
Pinedale stations
1
RSS3
2
RSS1
3
DB
4
DSSV
5
DSSB
amplitude (volts)
170
180
190
200
time (sec)

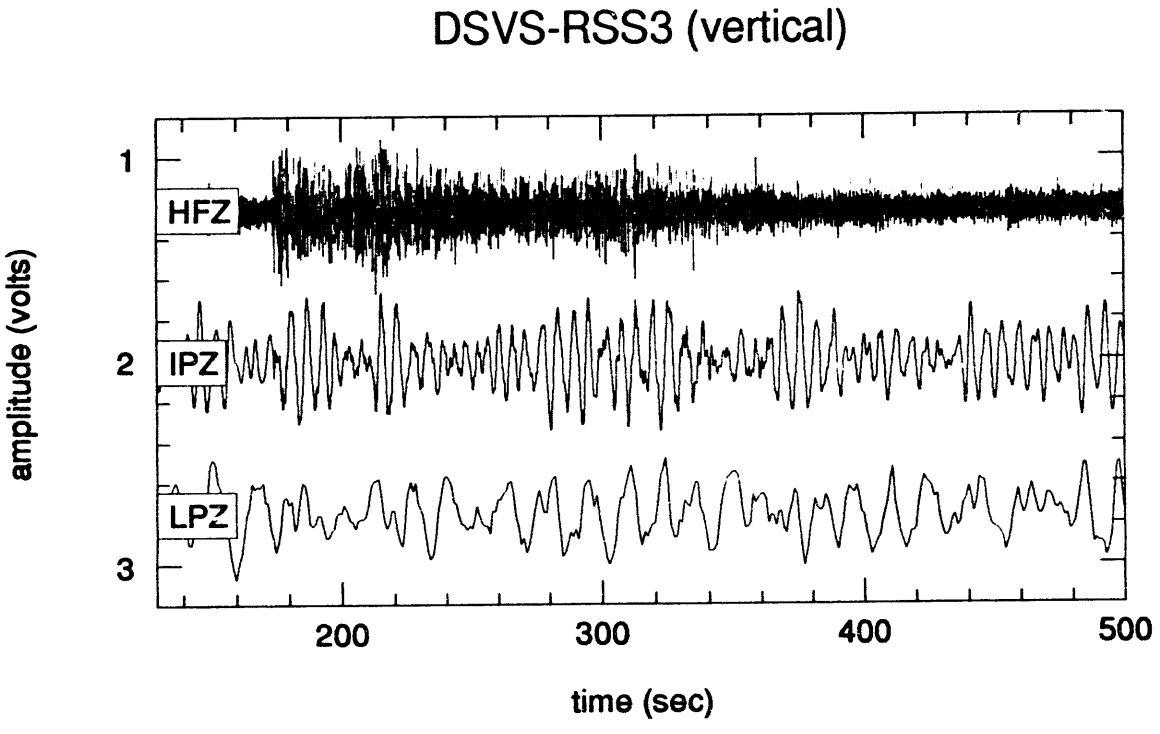
DSVS-RSS3 (vertical)
1
HFZ
2
IPZ
LPZ
3
amplitude (volts)
200
300
400
500
time (sec)

Fig 4

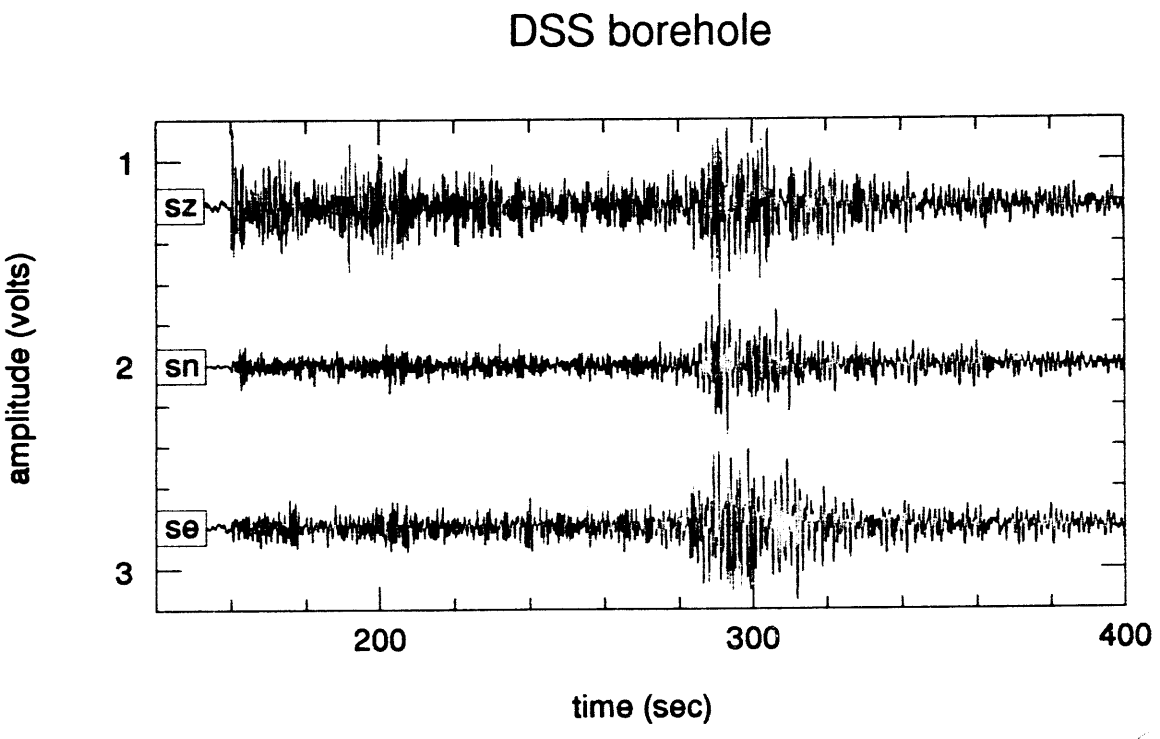
DSS borehole
amplitude (volts)
1
sz
2
sn
3
se
200
300
400
time (sec)

Fig 5

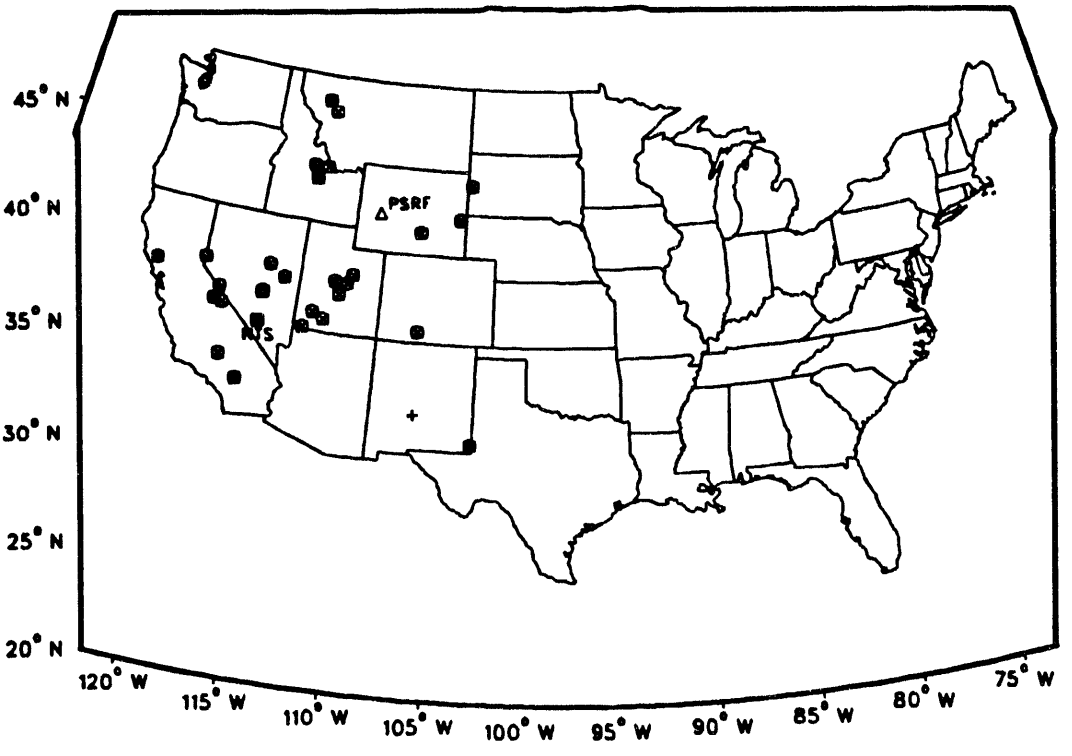
45° N
40° N
35° N
30° N
25° N
20° N
120° W
115° W
110° W
105° W
100° W
95° W
90° W
85° W
80° W
75° W
PSRF
NTS

Fig 6

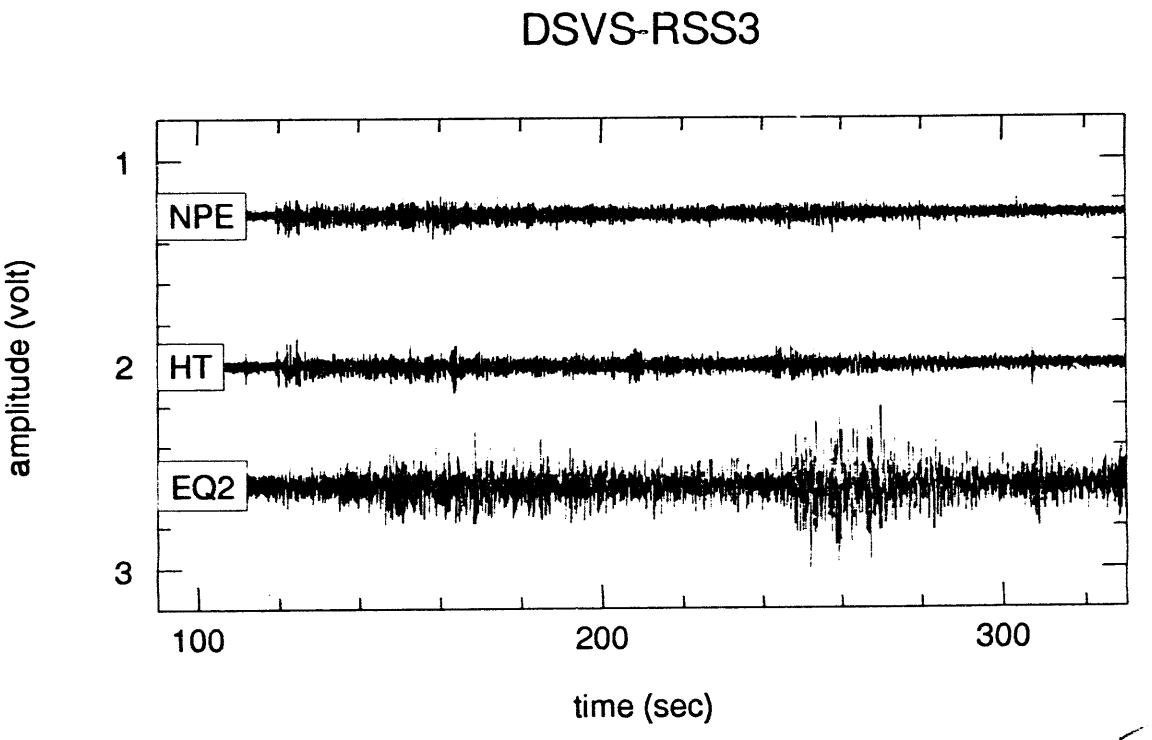

Fig 7

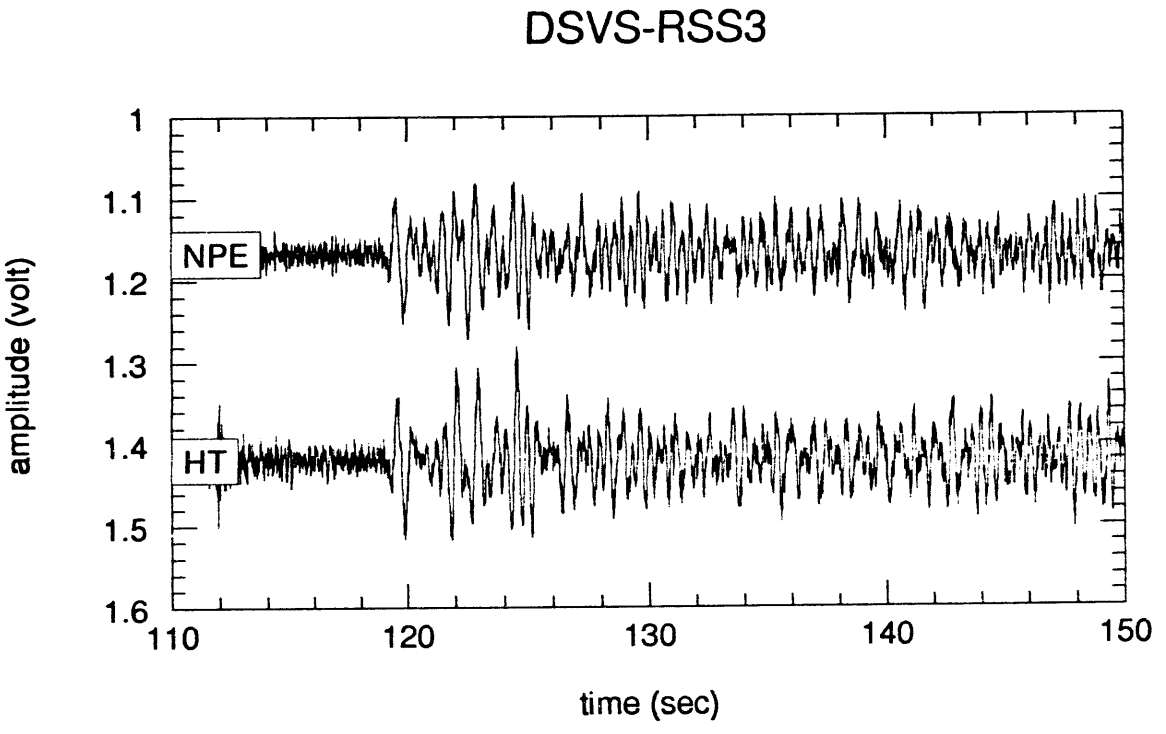
DSVS-RSS3
amplitude (volt)
1
1.1
1.2
1.3
1.4
1.5
1.6
NPE
HT
110
120
130
140
150
time (sec)

Fig 8

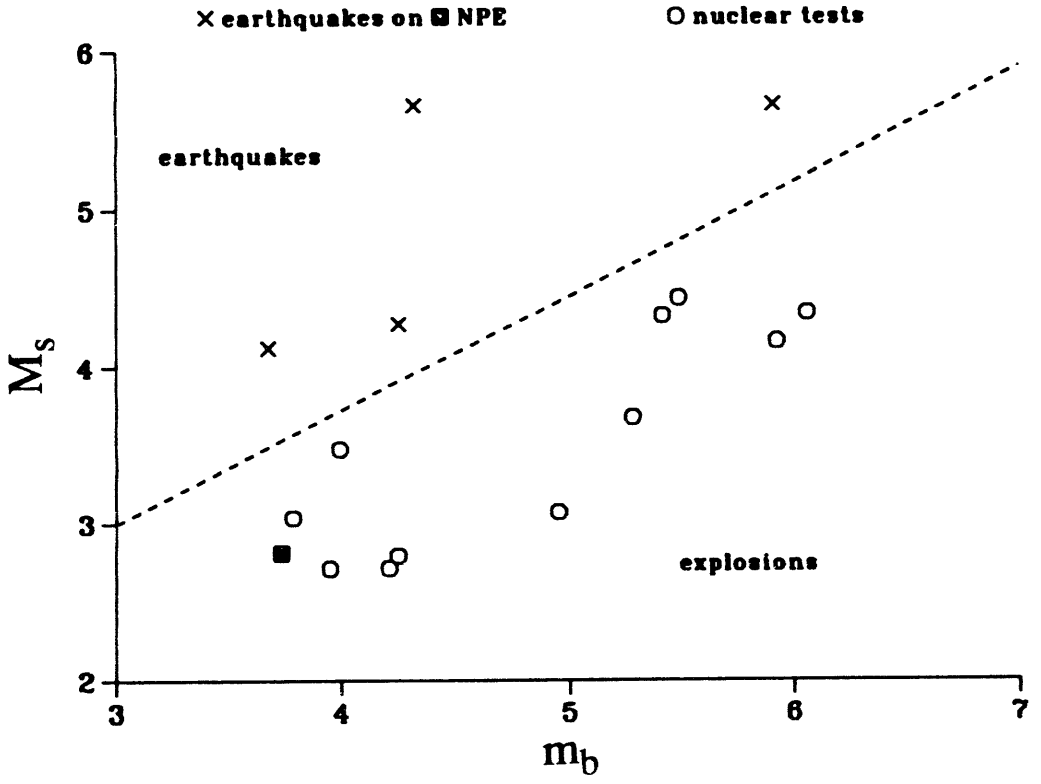
× earthquakes on ■ NPE
○ nuclear tests
earthquakes
explosions
M_S
m_b
6
5
4
3
2
3
4
5
6
7

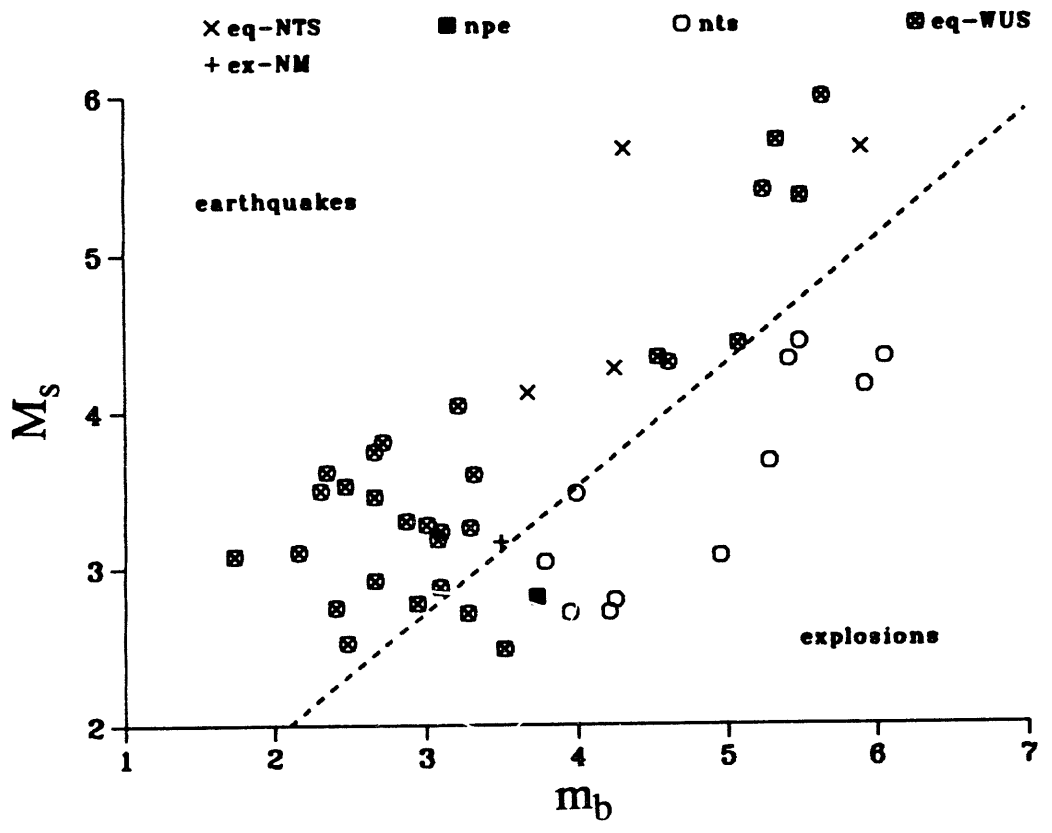
× eq-NTS
■ npe
○ nts
⊠ eq-WUS
+ ex-NM
earthquakes
explosions
M_S
m_b
6
5
4
3
2
1
2
3
4
5
6
7

Fig 10

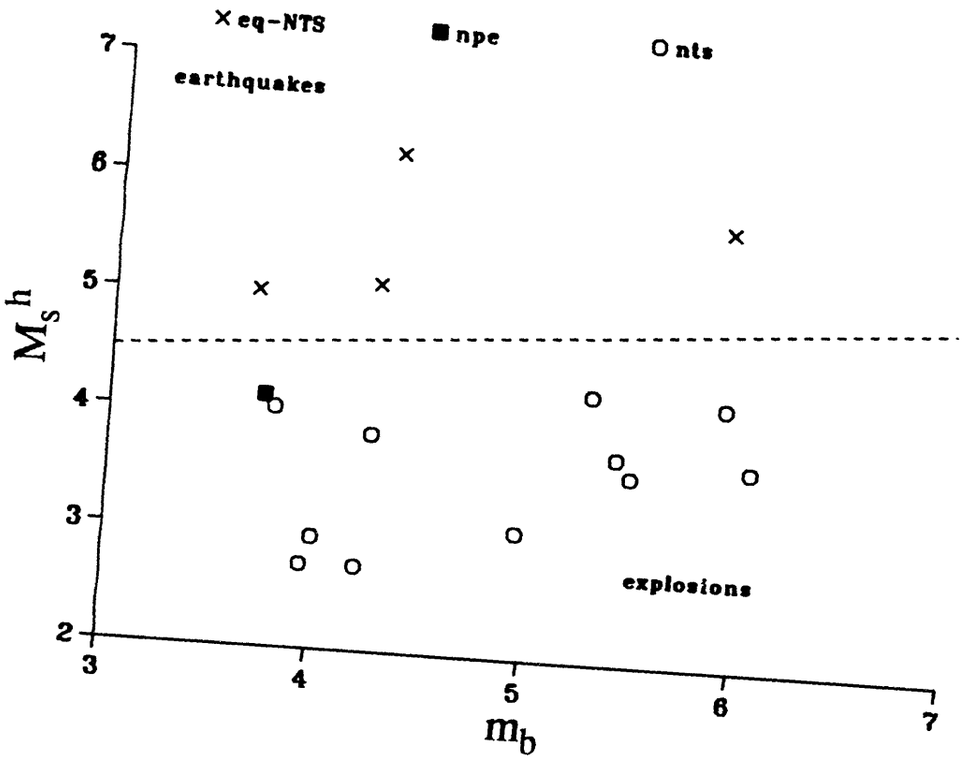
× eq-NTS
■ npe
○ nts
earthquakes
explosions
M_s^h
m_b
7
6
5
4
3
2
3
4
5
6
7

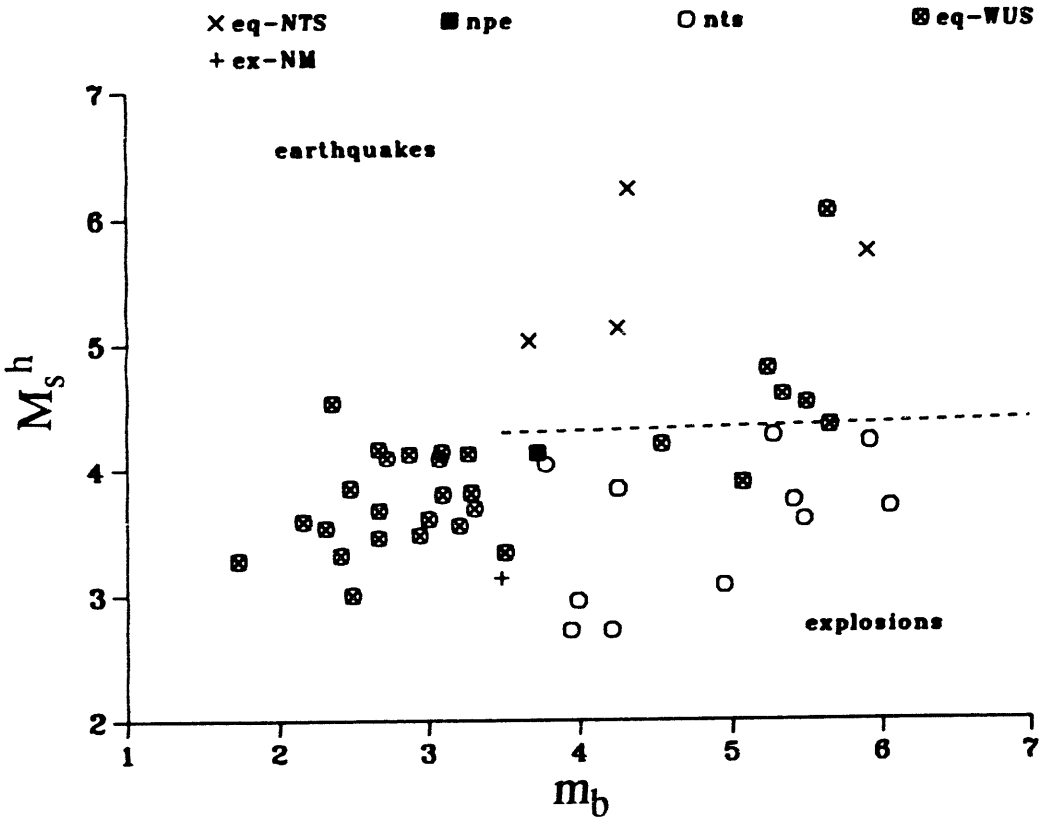
× eq-NTS
■ npe
○ nts
⊠ eq-WUS
+ ex-NM
earthquakes
explosions
M_S^h
m_b
7
6
5
4
3
2
1
2
3
4
5
6
7

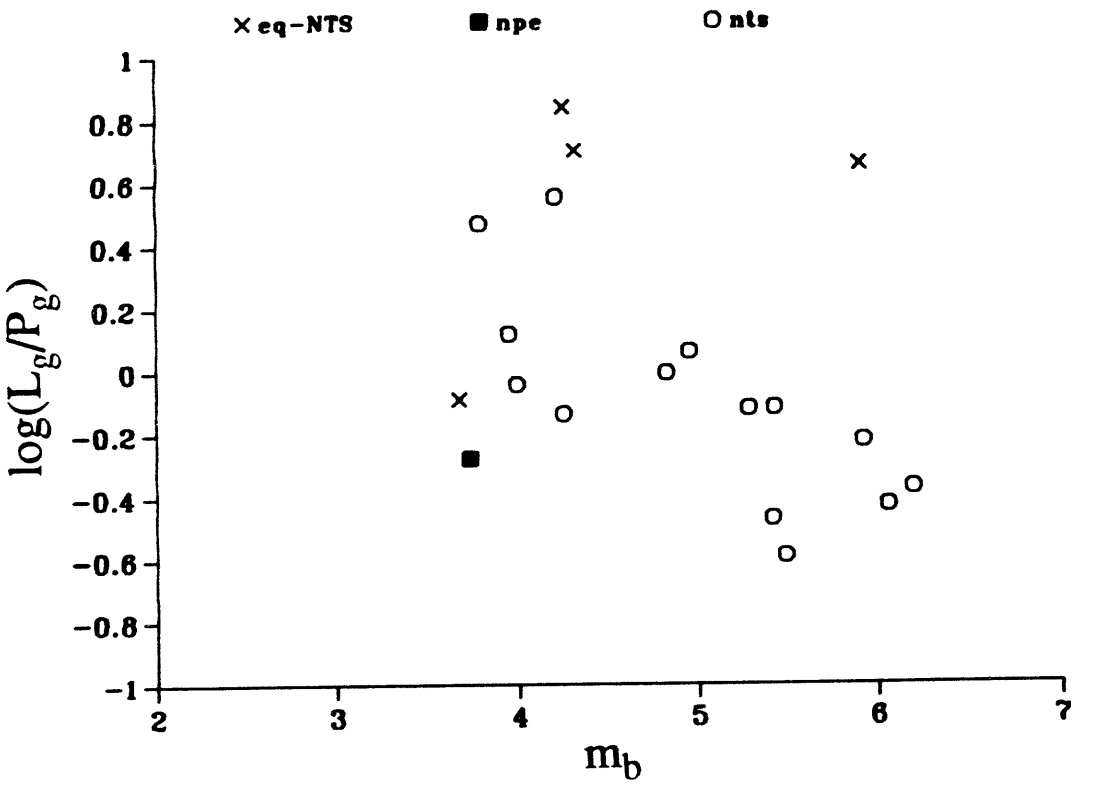
× eq-NTS
■ npe
O nts
1
0.8
0.6
0.4
0.2
0
−0.2
−0.4
−0.6
−0.8
−1
2
3
4
5
6
7
log(Lg/Pg)
mb

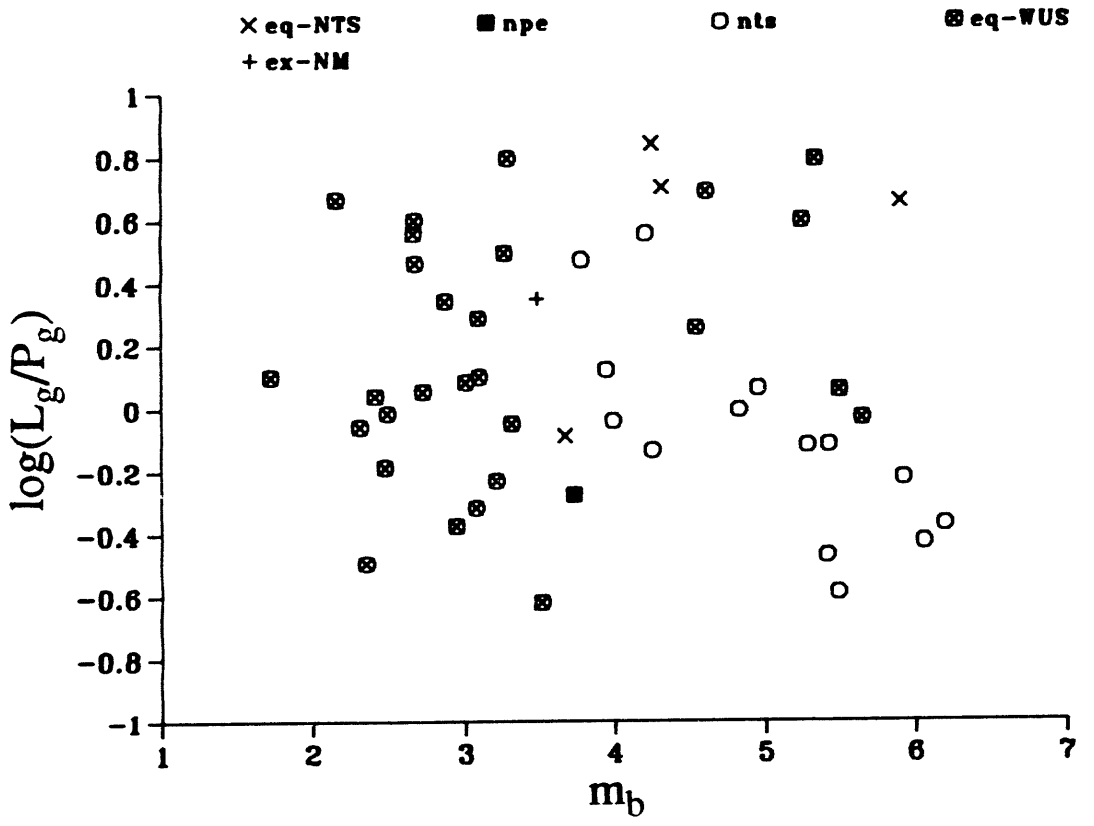
× eq-NTS
■ npe
○ nts
⊗ eq-WUS
+ ex-NM
1
0.8
0.6
0.4
0.2
0
−0.2
−0.4
−0.6
−0.8
−1
log(Lg/Pg)
1
2
3
4
5
6
7
mb

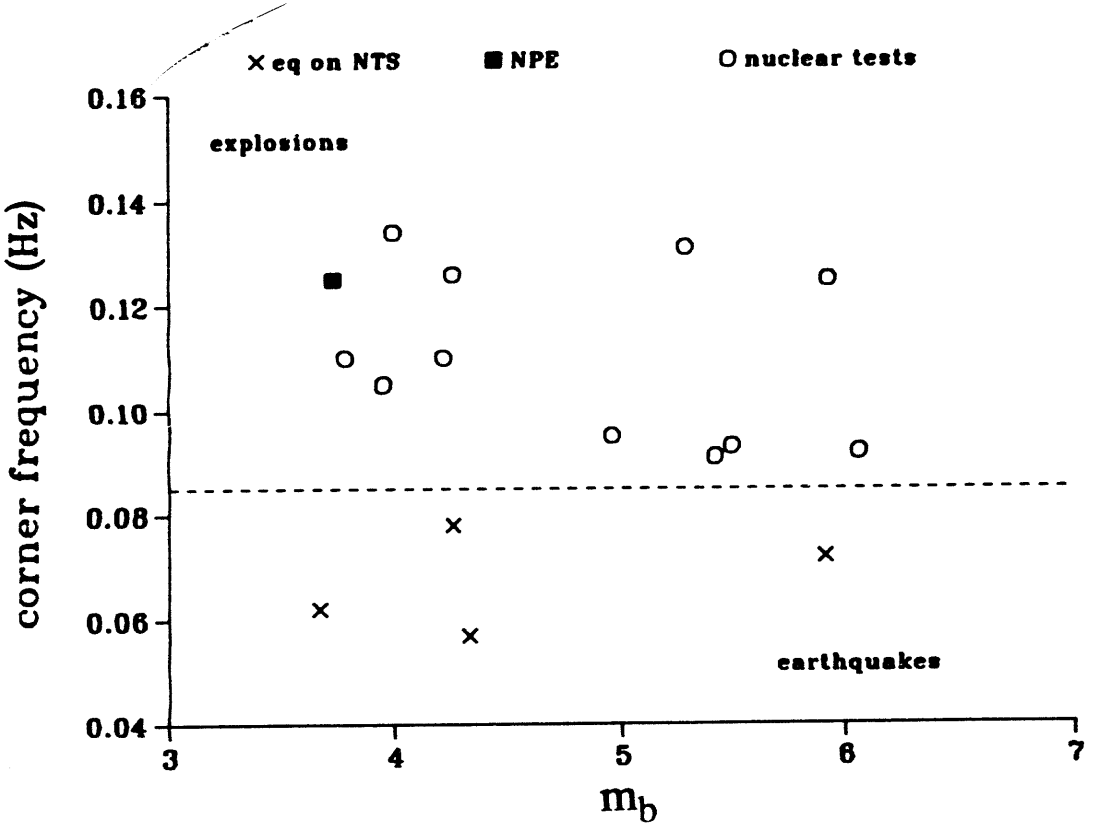
× eq on NTS
■ NPE
○ nuclear tests
explosions
earthquakes
corner frequency (Hz)
0.16
0.14
0.12
0.10
0.08
0.06
0.04
3
4
5
6
7
m_b

Fig 5

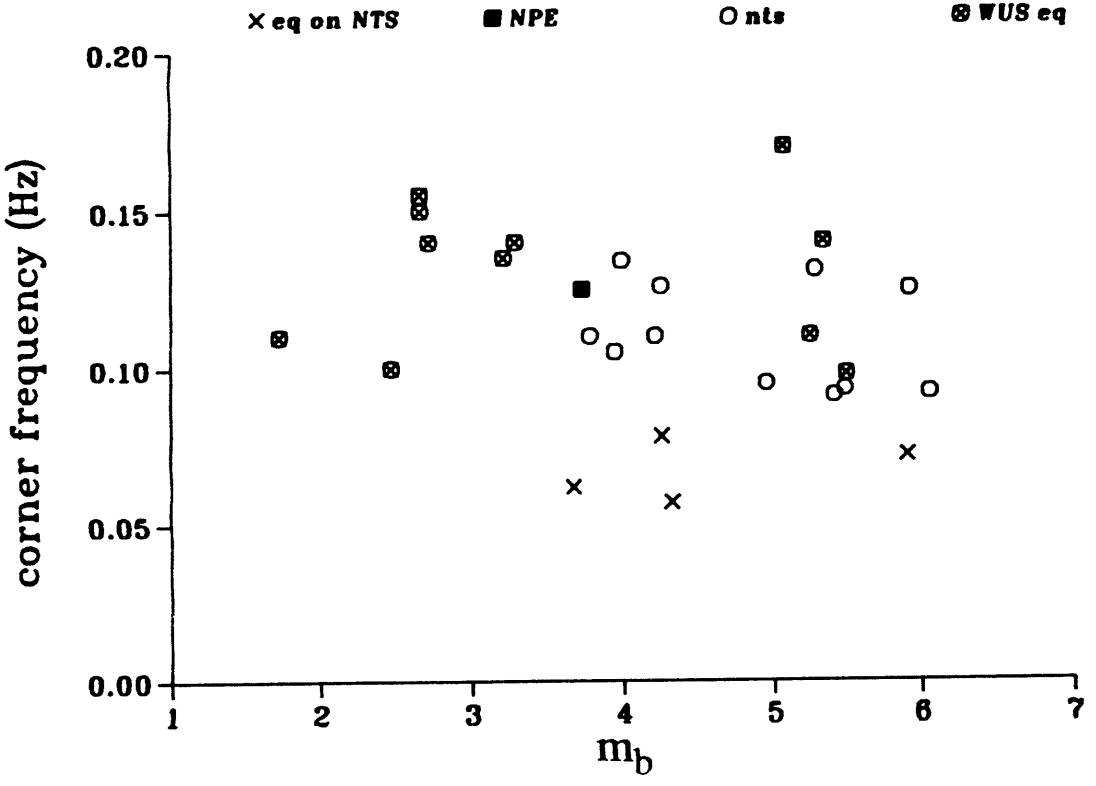
× eq on NTS
■ NPE
○ nts
⊗ WUS eq
corner frequency (Hz)
0.20
0.15
0.10
0.05
0.00
1
2
3
4
5
6
7
m_b

Fig 10

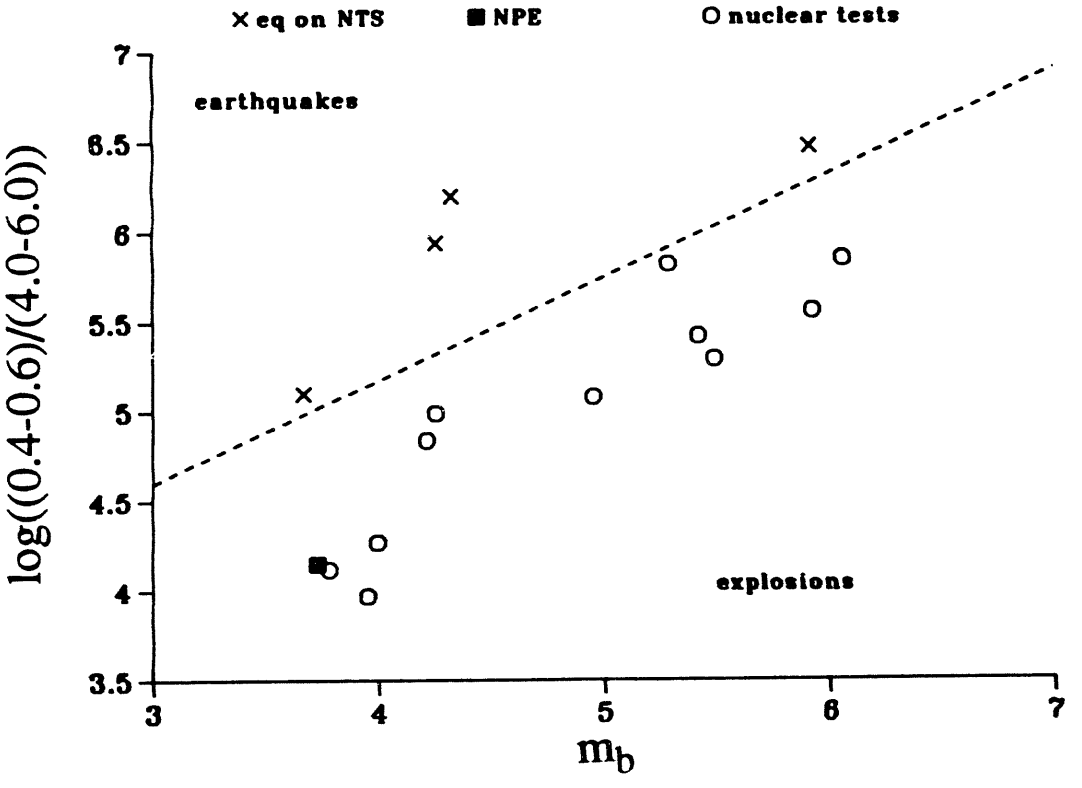
× eq on NTS
■ NPE
O nuclear tests
earthquakes
explosions
log((0.4-0.6)/(4.0-6.0))
7
6.5
6
5.5
5
4.5
4
3.5
3
4
5
6
7
m_b

Fig 7

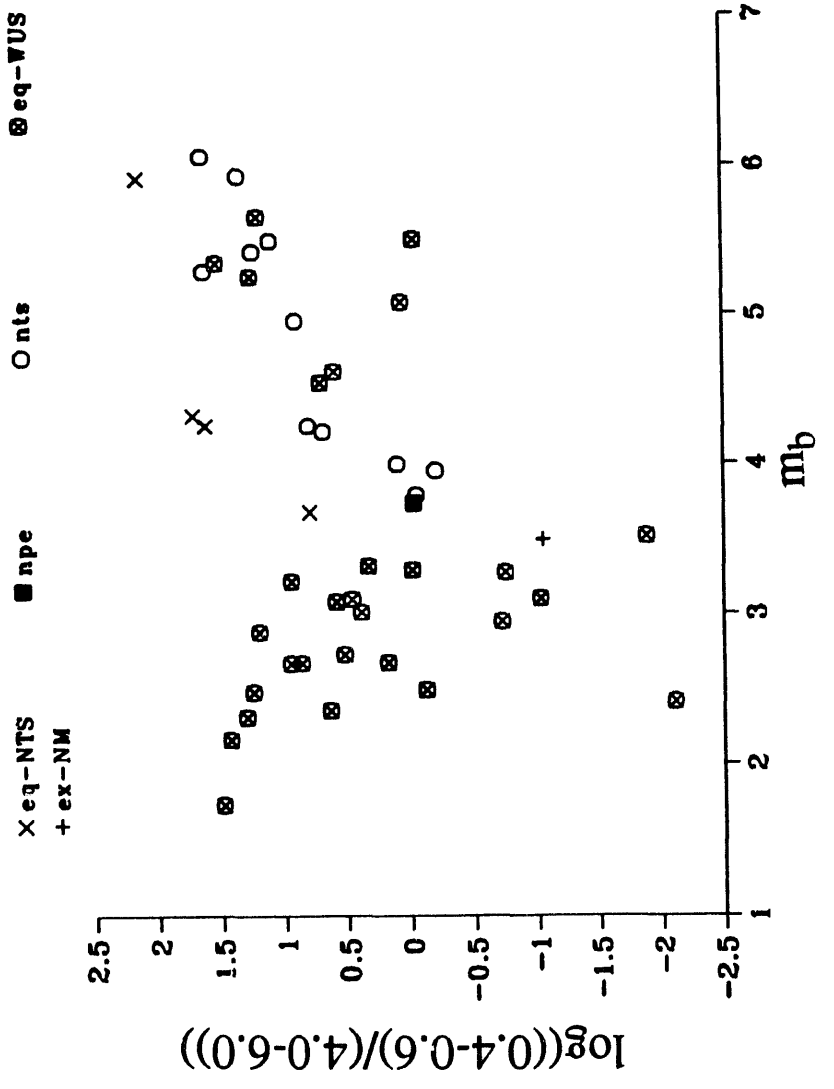

DISCLAIMER

DATE
FILMED
7/1/94
END